Superposition Model Analysis of Cr^{3+} Doped $TmAl_3(BO_3)_4$

Ram Kripal

EPR Laboratory, Department of Physics, University of Allahabad, Allahabad, India

Abstract: *Superposition model (SPM) is employed to find zero field splitting (ZFS) parameters (ZFSPs) and crystal field parameters (CFPs) of Cr^{3+} doped $TmAl_3(BO_3)_4$. Substitutional and structural vacancy sites for Cr^{3+} ion in $TmAl_3(BO_3)_4$ (TAB) crystal as well as distortion are considered for calculation. The evaluated ZFSPs agree well with the experimental values when distortion is taken into consideration. The optical energy band positions for Cr^{3+} in TAB are obtained using CFPs calculated from SPM and CFA package. The results show that Cr^{3+} ions substitute TAB lattice at Al^{3+} sites.*

Keywords: *Superposition model; Crystal field: zero-field splitting; Optical spectroscopy; Cr^{3+} ions in TAB.*

1. Introduction

The borates, $RM_3(BO_3)_4$, where R is the rare earth ions, and M is the Al, Fe, Ga and Cr ions, have various luminescent and non-linear optical properties making them valuable for research. For high concentrations of impurity ions in borates, no concentration quenching is there, as a result these crystals become promising systems for solid-state lasers [1–3]. Further, an opportunity to dope both rare earth and transition ions in these crystals makes them attractive for the magnetism studies [4, 5]. The magnetoelectric effect is also found [6, 7] in some crystals. Since the impurity ion doped in the crystals determines their properties, impurity location and crystal structure distortions produced are the subject of recent studies [8, 9].

Doping chromium in borate crystal generates safe radiation for eyes (425–675 nm) [10]. It can be reasonably expected that Cr^{3+} ions substitute for Al^{3+} since the Cr^{3+} ionic size (0.062 nm) is close to that of Al^{3+} (0.053 nm) [11–13]. EPR investigations of Cr^{3+} doped $TmAl_3$ $(BO_3)_4$ (TAB) single crystal at room temperature were carried out earlier [14]. To the best of our knowledge, no theoretical investigations of the zero field splitting parameters (ZFSPs) determined by EPR for Cr^{3+} doped TAB single crystal [14] have been performed as yet. The present paper deals with this theoretical investigation. To this end, the superposition model (SPM) is applied to perform theoretical analysis of the ZFSPs and the crystal field parameters (CFPs) for Cr^{3+} ions in TAB. The purpose is: (i) to find the ZFSPs for Cr^{3+} ions at all possible cation sites, (ii) to find the CFPs for Cr^{3+} ions and (iii) to understand the structural distortion around the substitutional Cr^{3+} ions at various cation sites. The optical energy band positions for Cr^{3+} in TAB are determined using CFPs and CFA package. The predicted ZFSPs and CFPs may be useful in future studies for technological applications of the huntite-type borates.

2. Crystal Structure

X-ray diffraction investigation shows that TAB crystal crystallizes in the huntite $[Mg_3Ca(CO_3)_4]$ structure with the space group R32. The hexagonal crystals have unit cell dimensions: a = 9.27050 Å, c = 7.21351Å and Z = 3 [14]. The trigonal prisms, octahedra and triangles formed by oxygen ions are coordination polyhedra of rare earth ions, Al^{3+} and B^{3+} ions, respectively. Rare earth ions are located on the rotary C_3 axis in slightly distorted prisms, where the top and bottom triangles are slightly turned relative to each other. The Al^{3+} ions are in oxygen octahedrons, which are coupled by edges and form twisted columns that are elongated along the C_3 axis. The B atoms are located in oxygen triangles of two types: in one type B atoms are in triangles perpendicular to the triple axes and alternate with Tm-prisms, and in other type B atoms are in triangles that connect the twisted columns from Al-octahedrons among themselves. Cr^{3+} ions preferentially substitute for Al^{3+} ions. The crystal structure of TAB is shown in Fig. 1. The local symmetry in TAB crystal is trigonal type I with the trigonal axis $C_3||c//z$ - for Al^{3+} sites. Due to doping of Cr^{3+} ion in TAB crystal, the site symmetry about Cr^{3+}ions is lowered and is taken to be approximately orthorhombic, as indicated by EPR spectra of Cr^{3+}: TAB at room temperature [14].

Since the crystallographic axis system (CAS), (*a, b, c*), is not Cartesian [29, 30], the modified crystallographic axis system CAS* (*a, b*, c*) is considered as shown in Fig. 1 (the axis *a* is perpendicular to *c* and *b**). A common axis system (*a//x, b*//y, c//z*) is taken to simplify our calculations.

The structural data in spherical polar coordinates for the Cr^{3+} sites in TAB on the basis of fractional positions of ligands [14] are shown in Table 1. These data are used for SPM/ZFS and SPM/CF calculations presented here for TAB: Cr^{3+}.

3. SPM Calculations of ZFSPs

The energy levels of transition ions doped in crystals are found by the spin Hamiltonian having electronic Zeeman (Ze) and ZFS terms [15, 16, 17]:

$$\mathcal{H} = \mathcal{H}_{\text{Ze}} + \mathcal{H}_{\text{ZFS}} = \mu_B B.g.S + \sum B_k^q O_k^q = \mu_B B.g.S + \sum f_k b_k^q O_k^q , \quad (1)$$

where g is the spectroscopic splitting factor, μ_B is the Bohr magneton, $\boldsymbol{B}$ is the applied magnetic field , S is the effective spin operator and $O_k^q(S_x, S_y, S_z)$ are the extended Stevens operators (ESO) [18, 19]. B_k^q and b_k^q are the related ZFSPs, f_k = 1/3 and 1/60 give the scaling factors for k = 2 and 4, respectively. The ZFS terms in (1) for Cr^{3+} ion with S = 3/2 at orthorhombic symmetry sites are found as [15, 16, 17]:

$$\mathcal{H}_{\text{ZFS}} = B_2^0 O_2^0 + B_2^2 O_2^2 = \frac{1}{3} b_2^0 O_2^0 + \frac{1}{3} b_2^2 O_2^2 = D(S_z^2 - \frac{1}{3} S(S+1)) + E(S_x^2 - S_y^2) \quad (2)$$

The conventional orthorhombic ZFSPs (D, E) and (B_k^q , b_k^q) are related as given below:

$$b_2^0 = D = 3\, B_2^0 \,,\; b_2^2 = 3E = 3\, B_2^2 \,. \quad (3)$$

Using SPM [20-22], the ZFSPs for a ML_n complex can be obtained (in ESO notation) for any symmetry as:

$$b_k^q = \sum_i \bar{b}_k (R_0) \left(\frac{R_0}{R_i} \right)^{t_k} K_k^q (\theta_i, \varphi_i) , \quad (4)$$

where (R_i, θ_i, φ_i) are the spherical polar coordinates of the i-th ligand. The intrinsic parameters $\bar{b}_k$ provide the strength of the k-th rank ZFS contribution from a ligand located at the distance R_i, whereas the coordination factors K_k^q give the geometrical information. K_k^q with k = 1 to 6 in the ESO notation obtained in [23] are retabulated in Appendix A1 of [24]. The distance dependence of the intrinsic parameters for a ML_n complex is given in (5) below [20-22, 24], where t_k are the power-law exponents and R_0 is the reference distance [24, 25-28].

Eq. (4) gives conventional ZFSPs, D and E as [24]:

$$b_2^0 = D = \frac{\bar{b}_2(R_0)}{2} \left[\left(\frac{R_0}{R_i} \right)^{t_2} \sum_i (3\cos^2\theta_i - 1) \right]$$

$$b_2^2 = 3E = \frac{b_2^2}{3} = \frac{\bar{b}_2(R_0)}{2} \left[\left(\frac{R_0}{R_i} \right)^{t_2} \sum_i \sin^2\theta_i \cos 2\varphi_i \right] \quad (5)$$

Cr^{3+} ion in TAB may be supposed to enter the lattice substitutionally at the Al^{3+} ion site, and the structural vacancy site having similar ligand arrangement. The local symmetry at Cr^{3+} ion site is considered to be approximately orthorhombic. In octahedral coordination of Cr^{3+} ion for $LiNbO_3$ having Cr^{3+}-O^{2-} bond, $\bar{b}_2(R_0)$ = 2.34 cm^{-1} and t_2 = -0.12 [29] have been used to find b_2^0 and b_2^2. Since Cr^{3+} ion in TAB has distorted octahedral coordination (Fig.1) with oxygens as ligands, the b_K^q in the present analysis are obtained using the parameters $\bar{b}_2(R_0)$ = 2.34 cm^{-1} and t_2 = -1.82.

The position of metal ion and spherical coordinates of ligands given in Table 1 are used for calculation. The conventional ZFSPs, D and E of Cr^{3+} ion in TAB crystal are found using (5). The reference distance of 0.110 nm was taken for the determination of ZFSPs [30], and the obtained values of conventional ZFSPs are |D| = 0.5328 $cm^{-1}$and |E| = 0.1235 cm^{-1}. The ratio b_2^2 / b_2^0 should be within the range (0, 1) for orthorhombic symmetry [31]. In the present investigation, the ratio $|b_2^2| / |b_2^0|$ = 0.695 and |E| / |D| = 0.221, which agrees with above for b_2^2 / b_2^0. However, the value of |E| does not agree with the experimental one. Therefore, with above values of t_2 and reference distance, the ZFSPs |D| and |E| are found for Cr^{3+} at the Al^{3+} site with distortion having position Al^{3+} (0.5569, 0.4280, -0.0724). The conventional ZFSPs obtained now are $|D|$ = 0.5291 cm^{-1}, $|E|$ = 0.0222 cm^{-1}, which are in reasonable agreement with the experimental values. The ratio $|b_2^2| / |b_2^0|$ = 0.125 and $|E| / |D|$ = 0.041 which is consistent with [31]. Further with above values of t_2 and reference distance, the conventional ZFSPs $|D|$ and $|E|$ are determined for Cr^{3+} at the structural vacancy site but the values found are much different from the

experimental ones. Hence, these data are not being presented here.

The calculated and experimental ZFSPs for Cr^{3+} ion doped TAB are shown in Table 2. From Table 2, it is observed that the conventional ZFSPs are in reasonable agreement with the experimental ones [14] when the distortion is taken into account.

4. SPM Calculations of CFPs

The CF energy levels of transition ions doped crystals [32-35], in terms of CF Hamiltonian $\mathcal{H}_{CF}$ [36, 37], using Wybourne operators [15,36], are given as:

$$\mathcal{H}_{CF} = \sum_{kq} B_{kq} C_q^{(k)} \qquad (6)$$

Employing SPM [20-22], the CFPs in (6) for a ML_n complex can be obtained as:

$$B_{kq} = \sum_i \bar{A}_k \left(\frac{R_0}{R_i} \right)^{t_k} K_{kq}(\theta_i, \varphi_i). \qquad (7)$$

where R_0 is the reference distance for the site; R_i, θ_i, φ_i are the polar coordinates of the i^{th} ligand and K_{kq} are the coordination factors [32]. To find B_{kq} (k = 2, 4; q = 0, 2, 4); $\bar{A}_2$ = 40, 400 cm^{-1}, t_2 = 1.3, $\bar{A}_4$ =11, 700 cm^{-1} and t_4 = 3.4 are taken [32]. The calculated B_{kq} parameters are given in Table 3. The ratio B_{22}/B_{20} = -0.097, which indicates that B_{kq} parameters are standardized [31]. Using B_{kq} parameters in Table 3 and CFA program [33, 34], the CF energy levels of Cr^{3+} ion in TAB crystals are found. The energy levels of Cr^{3+} ion are computed by diagonalizing the complete Hamiltonian containing the Coulomb interaction (in terms of the Racah parameters B and C), Trees correction, the spin-orbit interaction, the crystal field Hamiltonian, the spin-spin interaction and the spin-other orbit interaction. The computed energy values are given in Table 4. Since optical study report on Cr^{3+}: TAB could not be found in literature, the experimental energy values for isomorphous system Cr^{3+}: YAB [38] are given here for comparison. From Table 4, it is found that there is reasonable agreement between theoretical and experimental band positions. Thus the theoretical investigation of Cr^{3+} ions entering TAB lattice at Al^{3+} sites supports the experimental observation [38].

5. Summary and Conclusions

The zero-field splitting (ZFS) parameters (ZFSPs) and the crystal field (CF) parameters (CFPs) are obtained using superposition model (SPM) for Cr^{3+} ions in $TmAl_3(BO_3)_4$ (TAB) single crystals. Cr^{3+} ions entering the TAB lattice at Al^{3+} ion sites, structural vacancy site and distortion models are considered for computation. The calculated conventional ZFSPs for Cr^{3+} ion at Al^{3+} sites in TAB crystal are in reasonable agreement with the experimental values when distortion is taken into account for calculation. It is confirmed that the Cr^{3+} ions enter the lattice substitutionally at Al^{3+} ion sites. The CF energy values for Cr^{3+} ions at Al^{3+} sites obtained using CFA package and CFPs are in reasonable agreement with the experimental values. Thus the theoretical results support the experimental conclusion.

Acknowledgement

The authors are thankful to the Head, Department of Physics for providing the departmental facilities and to Prof. C. Rudowicz, Faculty of Chemistry, A. Mickiewicz. University, Poznan, Poland for CFA program.

References

[1] X . Chen, Z. Luo, D. Jaque, J. J. Romero, J. G. Sole, Y .Huang, A. Jiang and C. Tu, Comparison of optical spectra of Nd^{3+} in $NdAl_3(BO_3)_4$ (NAB), $Nd:GdAl_3(BO_3)_4$ (NGAB) and $Nd:Gd_{0.2}Y_{0.8}Al_3(BO_3)_4$ (NGYAB) crystals, J. Phys.: Condens. Matter 13(2001) 1171-1178.

[2] D. Jaque, O. Enguita, J. G. Sole, A. D. Jiang and Z. D. Luo, Infrared continuous-wave laser gain in neodymium aluminum borate: A promising candidate for microchip diode-pumped solid state lasers, Appl. Phys. Lett. 76 (2000)2176-2178.

[3] A. Brenier, C. Tu, Z. Zhu and B. Wu, Red–green–blue generation from a lone dual-wavelength $GdAl_3(BO_3)_4:Nd^{3+}$ laser, Appl. Phys. Lett. 84(2004) 2034-2036.

[4] A. D. Balaev, L. N. Bezmaternykh, I. A. Gudim, V. L. Temerov, S. G. Ovchinnikov and S. A. Kharlamova, Magnetic properties of trigonal $GdFe_3(BO_3)_4$, J. Magn. Magn. Mater. 258- 9(2003) 532-534.

[5] S. A. Kharlamova, S. G. Ovchinnikov, A. D. Balaev, M. F. Thomas, I. S. Lyubutin and A. G. Gavriliuk, Spin reorientation effects in $GdFe_3(BO_3)_4$ induced by applied field and temperature, J. Exp. Theor. Phys. 101(2005) 1098-1105.

[6] I. S. Lyubutin, A. G. Gavriliuk, V. V. Struzhkin, S. G. Ovchinnikov, S. A. Kharlamova, L. N. Bezmaternykh, M. Hu and P. Chow, Pressure-induced electron spin transition in the paramagnetic phase of the $GdFe_3(BO_3)_4$ Heisenberg magnet, JETP Lett. 84(2007) 518-523.

[7] A. K. Zvezdin, S. S. Krotov, A. M. Kadomtseva, G. P. Vorob'ev, Y. F. Popov, A. P. Pyatakov, L. N.

Bezmaternykh and E. A. Popova, Magnetoelectric effects in gadolinium iron borate $GdFe_3(BO_3)_4$, JETP Lett. 81(2005) 272-276.

[8] V. A. Chernyshov, A. E. Nikiforov and G. S. Slepuhin**,** Electronic structure of impurity Sm^{3+} centers in fluorite, Phys. Solid State 54(2012) 1445-1450.

[9] L. K. Aminov, A. A. Ershova, S. L. Korableva, I. N. Kurkin, B. Z. Malkin and A. A. Rodionov, Superhyperfine structure of the EPR spectra of Nd^{3+} and U^{3+} ions in Li*R*F$_4$ (*R* = Y, Lu, Tm) double fluorides, Phys. Solid State 53(2011)2240-2243.

[10] I. Cies´lik, J. Z. Mija, A. Majchrowski, M. Pe˛pczyn´ ska, P. Morawiak, M. Włodarski, Synthesis and characteristics of optical properties of crystalline YAl3(BO3)4: Cr,Ce, J. Achiev. Mater. Manufac. Eng. 48 (1) (2011) 24–28.

[11] R.C. Weast (Ed.), CRC Handbook of Chemistry, Physics, CRC Press, Boca Raton,1989, p. F187.

[12] L. Pauling, The Nature of the Chemical Bond, 3rd ed., Cornell University Press,Ithaca, N.Y., 1960.

[13] B.D. Stojanovic, V.R. Mastelaro, C.O. Paiva Santos, J.A. Varela, Structure study of donor doped barium titan ate prepared from citrate solutions, Sci. Sinter. 36 (2004) 179–188.

[14] A. A. Prokhorov, L. F. Chernush, T. N. Melnik, R. Minikayev, A. Mazur, V. Babin, M. Nikl, J. Lancok, A. D. Prokhorov, Optical and magnetic properties of the ground state of Cr^{3+} doping ions in $REM_3(BO_3)_4$ single crystals, Sci. Rept. 9(201912787(13 pages).

[15] C. Rudowicz, M. Karbowiak, Disentangling intricate web of interrelated notions at the interface between the *physical* (crystal field) Hamiltonians and the *effective* (spin) Hamiltonians, Coord. Chem. Rev. 287(2015) 28-63.

[16] C. Rudowicz, CONCEPT OF SPIN HAMILTONIAN, FORMS OF ZERO FIELD SPLITTING AND ELECTRONIC ZEEMAN HAMILTONIANS AND RELATIONS BETWEEN PARAMETERS USED IN EPR. A CRITICAL REVIEW, Magn. Reson. Rev. 13 (1987) 1-89; Erratum, C. Rudowicz, Magn. Reson. Rev. 13 (1988) 335.

[17] C. Rudowicz, S.K. Misra, SPIN-HAMILTONIAN FORMALISMS IN ELECTRON MAGNETIC RESONANCE (EMR) AND RELATED SPECTROSCOPIES, Issue 1,Appl. Spectrosc. Rev. 36 (2001) 11-63.

[18] C. Rudowicz, Transformation relations for the conventional O_k^q and normalised $O'_k{}^q$ Stevens operator equivalents with k=1 to 6 and $-k \le q \le k$, Number 7, J. Phys. C Solid State Phys. 18 (1985) 1415-1430; Erratum: C. Rudowicz, Number 19, J. Phys. C Solid State Phys. 18 (1985) 3837.

[19] C. Rudowicz, C. Y. Chung, The generalization of the extended Stevens operators to higher ranks and spins, and a systematic review of the tables of the tensor operators and their matrix elements, Number 32, J. Phys. Condens. Matter. 16 (2004) 5825-5847.

[20] D.J. Newman, B. Ng, Superposition model, Ch. 5 in: D.J. Newman, B. Ng (Eds.), Crystal Field Handbook, Cambridge University Press, 2000, pp. 83–119.

[21] D.J. Newman, B. Ng, The Superposition model of crystal fields, Rep. Prog. Phys. 52 (1989) 699-763.

[22] D.J. Newman, W. Urban, Interpretation of *S*-state ion E.P.R. spectra, Issue 6, Adv. Phys. 24 (1975) 793-844.

[23] C. Rudowicz, On the derivation of the superposition-model formulae using the transformation relations for the Stevens operators, Number 35, J. Phys. C: Solid State Phys. 20 (1987) 6033-6037.

[24] C. Rudowicz, P. Gnutek, M. Açıkgöz, Superposition model in electron magnetic resonance spectroscopy – a primer for experimentalists with illustrative applications and literature database, Appl. Spectroscopy Rev. 54 (2019) 673-718.

[25] M. Açıkgöz, A study of the impurity structure for $3d^3$ (Cr^{3+} and Mn^{4+}) ions doped into rutile TiO_2 crystal, Issue 2, Spectrochim. Acta A 86 (2012) 417-422.

[26] K.A. Müller, W. Berlinger, J. Albers, Paramagnetic resonance and local position of Cr^{3+} in ferroelectric $BaTiO_3$, Issue 9, Phys. Rev. B 32 (1985) 5837-5850.

[27] K.A. Müller, W. Berlinger, Superposition model for sixfold-coordinated Cr^{3+} in oxide crystals (EPR study), Number 35, J. Phys. C: Solid State Phys. 16 (1983) 6861-6874.

[28] M. Heming, G. Lehmann, Correlation of zero-field splittings and site distortions: Variation of b_2 FOR Mn^{2+} with ligand and coordination number, Issue 2, Chem. Phys. Lett. 80 (1981) 235-237.

[29] T. H. Yeom, Y. M. Chang, C. Rudowicz, Cr^{3+} centres in $LiNbO_3$: Experimental and theoretical investigation of spin hamiltonian parameters, Issue 3, Solid State Commun. 87(1993) 245-249.

[30] E. Siegel, K. A. Muller, Structure of transition-metal—oxygen-vacancy pair centers, Issue 1, Phys. Rev. B 19 (1979)109-120.

[31] C. Rudowicz, R. Bramley, On standardization of the spin Hamiltonian and the ligand field Hamiltonian for orthorhombic symmetry, Issue 10, J. Chem. Phys. 83 (1985) 5192-5197.

[32] Y. Y. Yeung, D. J. Newman, Superposition-model analyses for the Cr3+ 4A2 ground state, Issue 4, Phys. Rev. B 34 (1986) 2258-2265.

[33] Y. Y. Yeung, C. Rudowicz, Ligand field analysis of the $3d^N$ ions at orthorhombic or higher symmetry sites, Issue 3, Comp. Chem. 16 (1992) 207-216.

[34] Y. Y. Yeung, C.Rudowicz, Crystal Field Energy Levels and State Vectors for the $3d^N$ Ions at Orthorhombic or Higher Symmetry Sites, Issue 1, J. Comput. Phys. 109 (1993) 150-152.

[35] Y. M. Chang, C. Rudowicz, Y.Y. Yeung, Issue 5, Crystal field analysis of the $3d^N$ ions at low symmetry sites including the 'imaginary' terms, Computers in Physics 8 (1994) 583-588.

[36] B. G. Wybourne, Spectroscopic Properties of Rare Earth, Wiley, New York, 1965.

[37] B.N. Figgis, A. Hitchman, Ligand Field Theory; its Applications, Wiley-VCH, New York, 2000.

[38] J. P. R. Wells, M. Yamaga, T. P. J. Han, M. Honda, Electron paramagnetic resonance and optical properties of Cr^{3+} doped$YAl_3(BO_3)_4$, J. Phys.: Condens. Matter,15(2003)539-547.

Tables and Figure:

Table 1. Fractional coordinates of Cr^{3+} ion and spherical co-ordinates (R, θ, ϕ) of ligands in TAB crystal.

Position of Cr^{3+}	Ligands	Spherical co-ordinates of ligands		
		RÅ	θ^0	ϕ^0
ND: Substitutional	O(1)	4.5460	37.4	0
(0.5569, 0, 0)	O(2)	3.6152	3.9	0
	O(3)	4.3001	28.1	-48.9
	O(4)	6.2978	55.0	0
	O(5)	6.2978	124. 9	0
	O(6)	6.4066	53.6	0
WD: substitutional	O(1)	7.1714	54.8	-55.1
(0.5569, 0, 0)	O(2)	5.8168	44.7	-86.4
	O(3)	4.9239	28.7	68.2
	O(4)	6.2418	48.5	37.5
	O(5)	5.6059	123.3	37.5
	O(6)	6.3670	47.3	66.0

ND = No distortion, WD = With distortion.

Table 2. Calculated and experimental ZFSPs of Cr^{3+} doped TAB single crystal along with reference distance.

		Calculated ZFS parameters (cm^{-1})			Conventional ZFS parameters (cm^{-1})		
	R_0Å	$\lvert b_2^0 \rvert$	$\lvert b_2^2 \rvert$	$\lvert b_2^2 \rvert / \lvert b_2^0 \rvert$	$\lvert D \rvert$	$\lvert E \rvert$	$\lvert E \rvert / \lvert D \rvert$
ND	1.10	0.5328	0.3706	0.695	0.5328	0.1235	0.231
					0.5290[e]	0.0270[e]	0.051
WD	1.10	0.5291	0.0666	0.125	0.5291	0.0222	0.041
					0.5290[e]	0.0270[e]	0.051

ND = No distortion, WD = With distortion, Al^{3+} (0.5563, 0.4280, -0.0724)

[e] = experimental.

Table 3. B_{kq} parameters of Cr^{3+} doped TAB single crystal.

		Calculated B_{kq} (cm^{-1}) Parameters used for CFA package					
	R_0Å	B_{20}	B_{22}	B_{40}	B_{42}	B_{44}	$B22/B20$
WD	1.10	6149.723	-601.697	-61.6128	-203.135	-325.364	-0.097

WD = With distortion.

Table 4. Experimental and calculated (CFA package) energy band positions of Cr^{3+} doped TAB single crystal.

Transition from $^4A_{2g}(F)$	Experimentally observed band (cm^{-1}) [38]	Calculated energy band from CFA (cm^{-1})
$^2Eg(G)$	14641, 14695	14431,14644
$^2T_1g(G)$	15275, 15321, 15375	15935, 15979, 16310
$^4T_2g(F)$	16950	16709, 17074, 17153, 17284, 17407, 17529
$^2T_2g(H)$	20846	18150, 18445, 18650
$^4T_1g(F)$	23750	25265, 25516, 26234, 26456, 26888, 27033
$^2T_1g(aD)$		38299, 38390, 41133
$^2Eg(bD)$		41660, 42285

(Racah parameters in *A*, *B* and *C*, spin-orbit coupling constant and Trees correction are 0, 681, 2724 (= 4B), 276 and 70 cm^{-1}, respectively)

Figure. Crystal structure of $TmAl_3(BO_3)_4$.

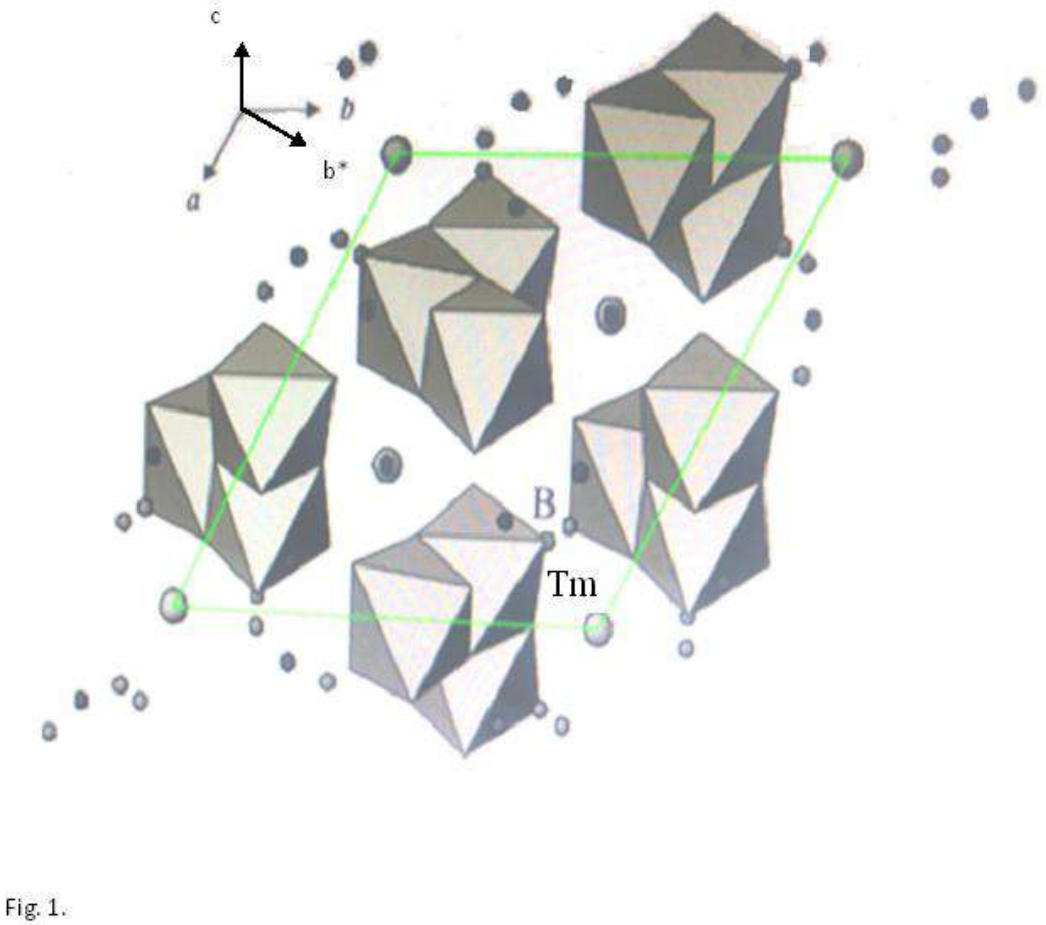

Fig. 1.

Fig1. Crystal structure of $TmAl_3(BO_3)_4$.